BUILDING PROTECTION AGAINST MULTIPLE HAZARDS

T.-C. PAN, B. LI, C. L. LIM, X. T. YOU AND K. W. CHENG
Protective Technology Research Centre, School of Civil and Environmental Engineering, Nanyang Technological University, Singapore 639798

ABSTRACT

Located off the southern tip of Malay Peninsula, Singapore is an island city-state. It has a land area of around 600 sq km and a population of about 3.2 millions. Although small in size, the country's gross domestic product per capita was about US$29,800 in 2002, among the highest in Asia. Most people live in high-rise residential buildings due to the land shortage. Being a metropolis with highly active trades and commerce, Singapore has also seen in recent years many modern high-rise commercial buildings constructed in her central business district.

This paper looks into the protective technologies for these modern high-rise residential and commercial buildings against multiple hazards. The hazards discussed here include both natural and man-made hazards. They are the effects resulting from the long-distance major Sumatra earthquakes, ground shocks induced by underground explosions, and blast loading from terrorist bombings. The consequences from any extreme event of the multiple hazards could be devastating to the society at large due to the high concentration of population as well as the high-value commercial and financial activities housed in these modern high-rise building structures.

1. INTRODUCTION

Although Singapore is believed to be located within the stable Sunda plate with mild winds, it is about 350 km away from an active earthquake belt, comprising the Great Sumatra Fault and the subduction zone of Sunda Trench. Singapore has never experienced any earthquake damage, and hence buildings are generally not designed against the horizontal earthquake loadings. However, tremors caused by distant Sumatra earthquakes have been felt in Singapore for many years. The seismic response of typical Singapore buildings to the maximum credible earthquakes from Sumatra will be discussed.

As part of the national effort to intensify the land use of the land-scarce country, Singapore has explored the possibility of using underground facilities for various purposes. One of initiatives is to move the surface ammunition storages underground, which will reduce the precious land surrounding the surface storages that have been sterilized for safety reasons. As a result, the dynamic response of building structures to ground shocks

that may result from underground explosions has been investigated. The results will be discussed in terms of the dynamic failure of RC buildings subjected to ground shocks, which in turn affects the minimum radial distance within which no residential buildings should be erected.

Recent terrorist bomb attacks around the world have demonstrated the ferocity, cruelty and unpredictability of the hazards posed by terrorism. Instead of trying to predict the next terror attack, it appears to be more important to protect critical assets like waterworks, seaports, airports, major buildings, etc. The transient dynamic response of a high-rise commercial building to a postulated external explosion load resulting from terrorist bombing will be discussed.

2. SEISMOTECTONICS OF SUMATRA AND THE MCE EVENT

Sumatra is located adjacent to the Sunda trench, Figure 1, where the Indian-Australian plate subducts beneath the Eurasian plate at a rate of 67 ± 7 mm per year towards N11°E ± 4° (Tregoning et al, 1994). The islands of Sumatra and Java lie on the over-riding plate, one hundred some kilometres from the trench. Convergence is nearly orthogonal to the trench axis near Java, but it is highly oblique near Sumatra, where the strain is strongly partitioned between the dip slip on the subduction zone interface and the right-lateral slip on the Sumatran fault along the western coast of the island. Large earthquakes have thus been generated in the region. The largest subduction earthquake that has occurred in the Sunda trench is the great 1833 event with an estimated Mw between 8.8 and 9.2 (Zachariasen et al, 1999). The earthquake, with an average Mw of 9.0 with an epicentral distance of 723 km, is thus selected for this study to be the maximum credible earthquake (MCE) that the Sumatra subduction zone is capable of generating (Megawati and Pan, 2002). The larger of the two horizontal components of the synthetic MCE ground motions is used in the convolution process to obtain the surface accelerations at a soft soil site.

3. SITE RESPONSE ANALYSIS

The soft soil site located at Katong Park (KAP) along the south-east coast of the Singapore island is used for site response analysis. The site is on Kallang Formation which consists of late Pleistocene and recent deposits of marine, alluvial, littoral and estuarine origin. The most important unit of the Kallang Formation is the marine clay. It occurs over an area covering one quarter of the island, but no surface outcrops exist. Its thickness is extremely variable with a maximum recorded of 35 m (Pitts, 1984). The subsurface profile of the KAP site consists of 6.5 m of fill material, followed by the 24 m of marine clay unit. The marine clay unit consists of upper and lower members separated by a weathered crust on top of the lower member. The equivalent linear site response analysis is carried out for the soft soil site using the MCE ground motions, using the EERA program (Bardet et al, 2000), of layered soil deposits. The simulated surface acceleration time-

history and its Fourier and response spectra for the MCE event are shown in Figure 2.

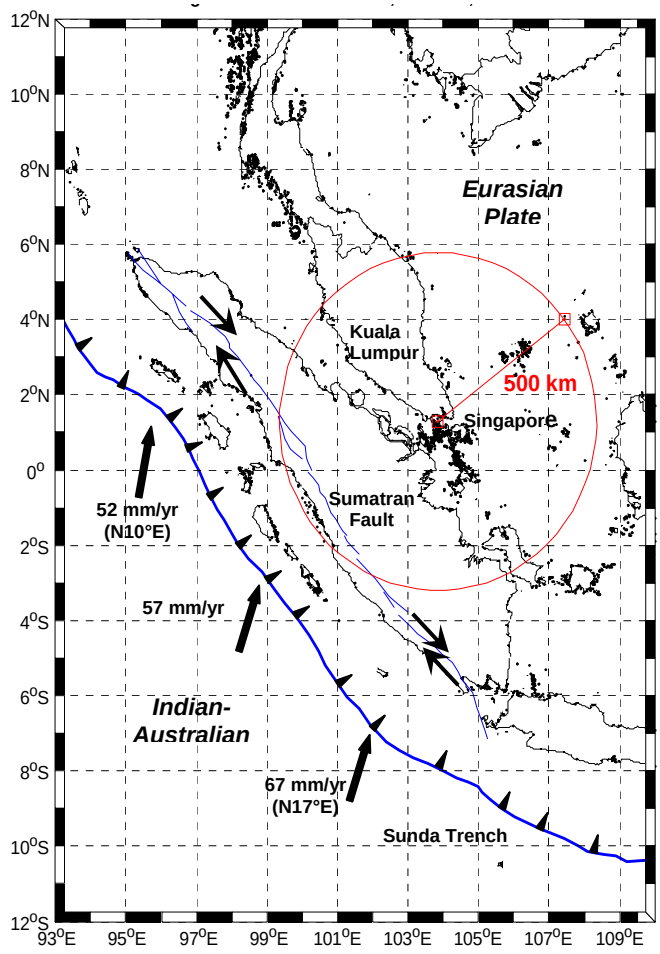

Figure 1: Seismotectonics of Sumatra region

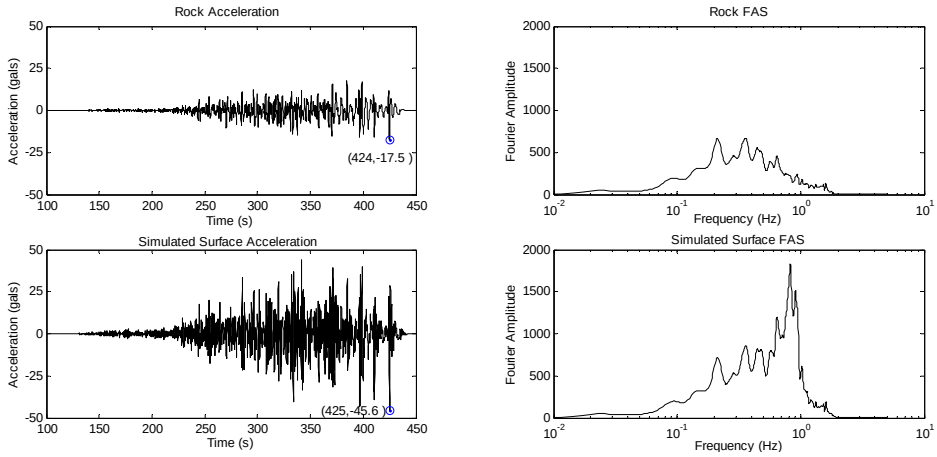

Figure 2: Acceleration time-histories and Fourier spectra for the maximum credible earthquake at rock and soft soil sites

4. BUILDING RESPONSE TO THE MCE EVENT

The elastic responses of a typical high-rise residential building subjected to the MCE earthquake are studied. Both the rock and the soft soil site ground motions are used as the inputs. The typical building is a 15-storey, reinforced concrete (RC) residential building. The overall height of the building is 42.8 m, with the first storey of 3.6 m and the others 2.8 m. The dimensions of the floor plan are 94.5 m in the longitudinal direction and 11 m in the transverse direction. The lateral load resistant system of the building is a RC frame-shear wall dual system. The frame system consists of a series of two-bay frames spanned in the transverse direction, with 3 m spacing between frames along the longitudinal direction. The typical column sections are 0.3 m by 1.2 m for the first three stories, and 0.3 m by 0.9 m for the upper stories, with the larger dimension the building's transverse direction. The typical beam size is 0.3 m by 0.5 m. The shear walls are around the three staircases located towards the ends and the middle of the building. The thickness of the wall panels is 0.2 m. Most of the walls are also aligned along the transverse direction of the building. Therefore, the longitudinal direction of the building is softer than the transverse direction. The RC frames are generally infilled with clay brick partition walls, except the ground storey where it is left open for public usage. The floors are cast-in-situ RC slabs of 0.125 m thickness. Because of the large aspect ratio of the floor dimensions, the effects of flexible diaphragms on included in the building's seismic response using shell elements.

The perspective view of the model is shown in Figure 3. In the model, the brick partition walls were ignored. The fundamental frequency of the model is 0.56 Hz. Figure 4 shows the first 5 mode shapes of the model. As shown, the first 4 modes are primarily the global translational or rotational modes, where the diaphragms behave rigidly. However, mode 5 is clearly a diaphragm deformation mode where the floors are bent as a flexible beam. The ground motions are applied separately in the longitudinal and the transverse directions. The time history results of the total base shear forces are obtained. The maximum base shear force resulting from the soft soil site response to the MCE event is about 2.16E+04 kN, which is 13.9% of the total building dead weight. This maximum base shear force ratio exceeds the notional horizontal load specified in the local code as 1.5% of the characteristic dead weight of the building.

5. RESPONSE TO GROUND SHOCKS

Explosion-induced ground motions (EIGMs) or ground shocks could be one of the possible damaging ground motions to be faced in the lifetime of a structure owing to accidental or intentional explosions. However, since ground motions of earthquakes and EIGMs are inherently different, direct application of earthquake engineering principles to ground shock cases may be questionable. By subjecting a lightly-reinforced RC frame to a simulated

EIGM, the suitability of current earthquake design philosophies and damage assessment techniques for EIGMs is investigated in this section.

EIGM characteristics can be segmented into two parts: the major shock duration (Phase I) and the ensuing duration (Phase II). Dhakal and Pan (2003) showed that the high frequency nature of an EIGM led to a large shear force with small deformation during Phase I followed by significant deformation in Phase II. Other studies have shown that the EIGM produces significant local damages owing to the high frequency content of EIGMs (Ma et al, 2002). In this paper, impulse per unit mass of a ground motion is used as a gauge of the damaging potential of the ground input.

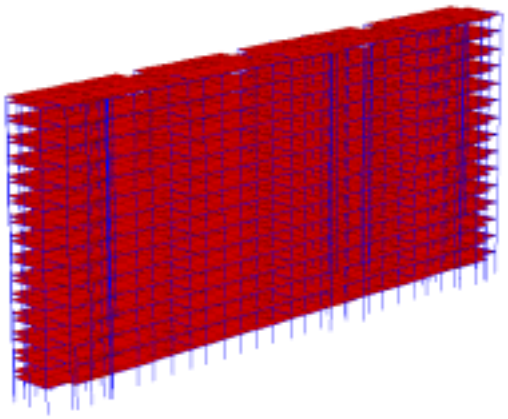

Figure 3: Perspective view of the FE model

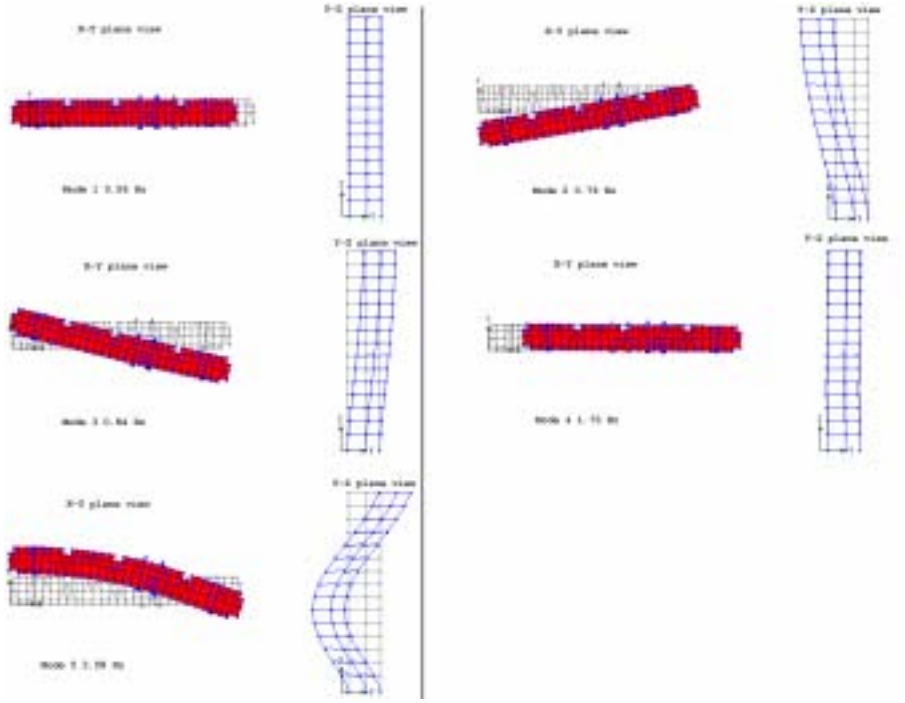

Figure 4: The first 5 mode shapes of the FE model

5.1 Member and joint strengths

Member strength includes flexural and shear strengths, respectively. While the predictive flexural strength equation stated in (Park and Pauley, 1974) has been widely accepted, there is less confidence on the existing shear strength predictive equations (ASCE-ACI, 1973, Karim, 1999, Priestley et al, 1994). Shear strength has been regarded to comprise contributions from concrete and steel reinforcement. With variations of the steel contribution, these predictive equations state a similar concrete contribution (Karim, 1999, Priestley et al, 1994). For the small deformation in Phase I, the contribution of the longitudinal reinforcement to the member shear strength may not be significant. Thus, the shear strength of members during Phase I would mainly be contributed by the concrete strength.

Observations of the buildings damaged during the strong Chilean earthquakes of the 1960's showed damage in the beam-column joints (i.e. joint panels). Joints act to transfer forces between beams and columns, and so their state reflects the extent of the load transfer mechanism. Joint performance has been observed to be dependent on joint shear strength (Paulay and Priestley 1978). When the joint shear strength is exceeded, member strengths will be compromised. For a non-seismically designed joint, joint cracking and joint failure were observed at a 0.5% and 3% inter-storey drift ratios, respectively (Pan et al 2001, Li et al 2003).

5.2 Post-elastic response and damage assessment

Hysteretic models attempt to describe the post-elastic behaviour of RC members in terms of hysteretic energy dissipated. The advantage of using hysteretic model of members over material model is its lower computational effort. Park and Ang (1985) proposed a three-parameter post-elastic model where the post-elastic behaviour of members is described by stiffness degradation, strength deterioration and pinching parameter. In earthquake response analysis, damage assessment techniques provide qualitative information of structural performance under earthquake actions. Damage assessment techniques may be classified as strength-based, response-based or the hybrid of the two. Of the many damage assessment techniques, the hybrid damage assessment technique by Park and Ang (1985) is widely used. The damage levels were categorized as moderate, severe and partial or total collapse.

5.3 Response to a simulated EIGM

A non-seismically designed 6-storey RC frame was subjected to a simulated EIGM. The RC frame and the details are shown in Figure 5. The simulated EIGM is similar to that used in (Ma et al, 2002) for the horizontal ground motion at a distance from the explosion source. The simulated EIGM has a peak ground acceleration (PGA) of 124 g and a predominant frequency of about 200 Hz, Figure 6.

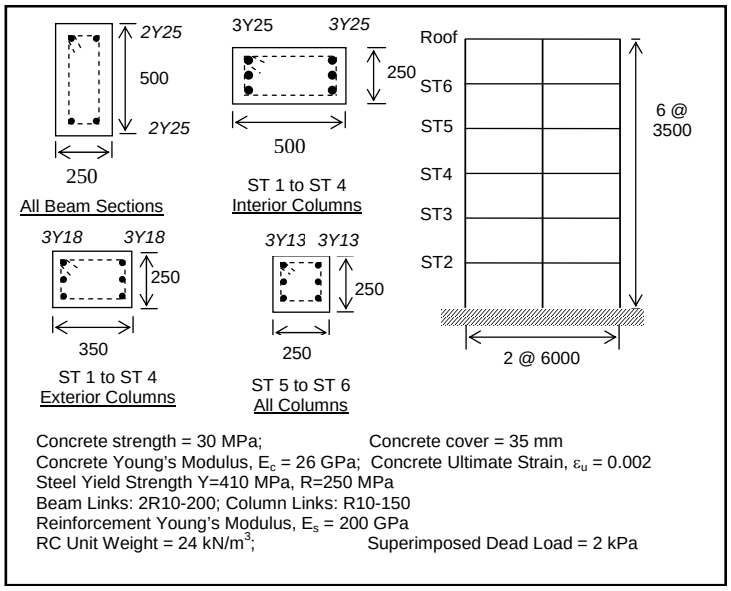

Figure 5: RC frame elevation and details

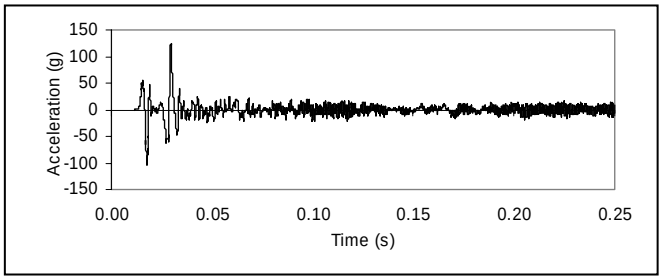

Figure 6: Horizontal acceleration time history of a simulated EIGM

The IDARC software (Valles et al, 1996) with Park and Ang's three-parameter hysteretic model and damage assessment procedure was used for analysis. For a qualitative understanding of the generic damage assessment techniques, local mode responses described in Ma et al (2002) were not modelled, while 3% inter-storey drift ratio was used as the joint failure criterion. The shear failure occurs when the nominal shear stress exceeds the shear strength predicted in Priestley et al (1994).

The Phase I responses of different storey levels (ST) are: the maximum roof displacement 12 mm; the peak inter-storey drift ratio 0.29% reached at ST2, and the maximum storey acceleration 1.36 g at ST2. The largest nominal shear stress occurred at the base of interior column, which was below shear strength. The damage level was moderate according to Park and Ang's model. The Phase II response exhibited a much larger deformation. The largest roof displacement was 230 mm, and ST6 had the largest inter-storey drift ratio of 3.2% (i.e. joint failure). The maximum nominal shear stress occurred at the base of interior column without shear failure. For this column, there was flexural yielding. However, the damage level was identified as moderate. Therefore, such a damage level does not reflect the actual damage associated with the joint failure.

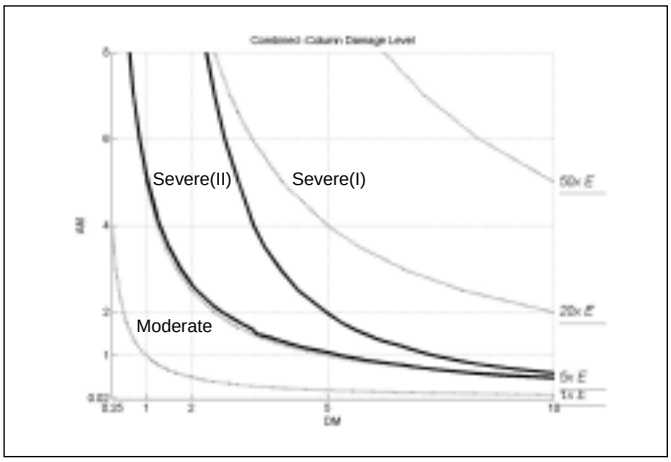

Figure 7: Zones of failure patterns for different response phases

5.4 Failure analysis

To understand the effects of the duration and the input impulse of EIGMs, duration multipliers (DM) and amplitude multipliers (AM) were applied on the above EIGM. The main parameters investigated are the predominant frequency and the amount of energy. Following this procedure, the response analysis and damage assessment of the 6-storey RC frame subjected to a family of scaled EIGMs were performed. Both shear failure and joint failure were investigated for the first storey interior column where the maximum shear stress occurred.

Combinations of DM and AM can lead to joint and/or failure in Phase I or Phase II. The damage level for the first storey column is presented in Figure 7. One bold line shows the boundary between the moderate and the severe damage levels for Phase I, Severe (I). The other bold line shows the boundary between the moderate and the severe damage levels for Phase II, Severe (II). Iso-impulse lines are shown as dotted lines in the background.

The figure shows that the iso-impulse line of 1xE produced moderate damage in both Phases I and II. A scaled EIGM with a DM=1 and AM=2 produced a moderate damage level. Therefore, it can be seen that the damage level as computed does not reflect adequately the shear failure and joint failure caused by this scaled EIGM.

6. RESPONSE TO EXTERNAL EXPLOSIONS

Effects of an external explosion on a high-rise commercial RC building resulting from a vehicle bomb at the ground level near the building are investigated in this section. The standoff distance is qualitatively classified as long or short. The high-rise commercial building selected for the study is a 30-storey RC structure with frames and a shear wall core. The building structural system consists of one storey of basement, 9 storeys of shopping centres cum car park, one mechanical floor and 20 storeys of

office space, Figure 8. It is about 146.5 m high, and the typical floor plan from the 10th storey upwards is 29 m x 44 m. Some beams and all floor slabs are post-tensioned RC members.

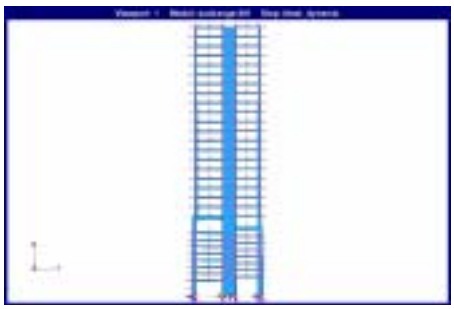

Figure 8: FEM model of the building

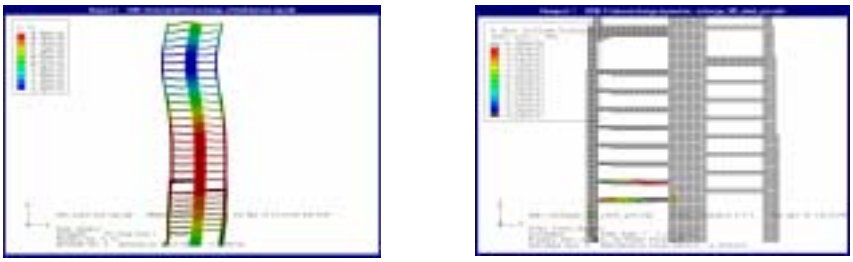

Figure 9: Deformation and stress distributions of the long standoff case

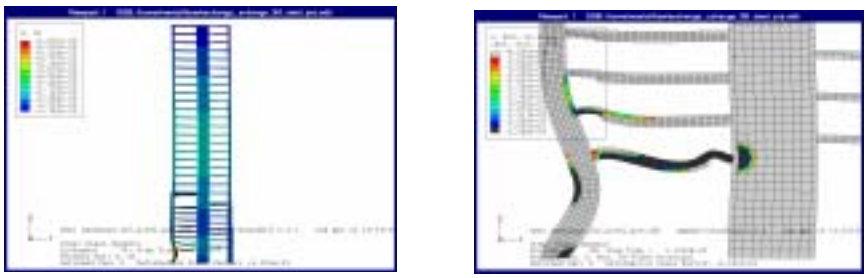

Figure 10: Deformation and stress distributions of the short standoff case

6.1 Blast load and FEM modelling

The parameters defining the blast loading characteristics are the peak pressure and loading duration, which can be determined using ConWep (Hyder, 1991). The distribution of the blast loading is non-uniform along the building height and varies with the explosive weight and the standoff distance. A typical plane frame of the building was analyzed. 2D solid continuum element with 4 nodes was used to model the concrete, and rebar element was merged with the solid concrete element (ABAQUS, 2001). The cap plasticity model was used to represent the concrete behaviour under blast load, while the elasto-plastic model was used for rebars. The dead and the live load were first applied prior to the dynamic analysis of building response to surface blast load.

6.2 Blast response evaluations

6.2.1 Long standoff case

The building deformation at a representative time step of the long standoff distance case is shown in Figure 9. The lateral displacement of the blast-loaded bottom column reaches its peak at 13.4 ms. Plastic deformation was mainly concentrated at the bottom column and the beams of the second and the third storeys. Most severe damage appeared in the column around 13 ms and in the beam around 16 ms. The beam deformation was focused at its ends where local damages occurred. Shear wall played an important role in the global response and exhibited a lateral vibration beginning around 30 ms resulting from the force transferred from the beams. The lateral vibration propagated upwards and reached the roof level around 200 ms.

The maximum tensile and crushing stress of concrete are assumed to be 1.7 MPa and 25 MPa, respectively. The cracks would first occur in the shear wall and propagate towards the upper part of the building. At 3 ms, crushing of concrete first occurred at one corner of the fixed-end column and at the left ends of the second and the third storey beams. As the compressive wave propagated to the other end of the beams, the second storey beam was almost completely crushed. Crushing of concrete in the shear wall was confined to its connection with the second storey beam.

The local damage index based on curvature is used to evaluate the flexural performance of structural elements under blast load. The second and the third storey beams were nearly in complete failure. Sever damage appeared in columns on the first and the second storeys and in the beams at the fourth and the fifth storeys.

6.2.2 Short standoff case

The building deformation at a representative time step of the short standoff distance case is shown in Figure 10. The lateral displacement reaches its peak value at 13.3 ms. The dynamic deformation was localized at the blast-loaded columns between the first and the third storeys. The beams connected with these columns might thus be damaged. Large residual deformations were observed for the blast-loaded columns and the beams connected to them. Compared with the long standoff case, the global response of the short standoff case hardly existed.

Extensive cracks first occurred in the blast-loaded bottom column. The cracks propagated sideways via the shear wall to the bottom column on the other side of the building as well as upwards in the wall. At 300 ms, the crack reached the roof. In addition, cracks also appeared in the transfer girders located at the tenth storey as a large tensile stress propagated through them. Compared with the long standoff case, the cracks in the concrete columns in the short standoff case were more severe, while those in the shear wall were less severe. At 1.5 ms, concrete crushing first appeared at the right corner of the lower end of the bottom column. The crushing zone developed towards the central zone of the column. In addition, the concrete

at the compressive zone of the second and the third storey beams was severely damaged.

Figure 10 shows that partial collapse or moderate damage may exist in the columns on the first and the second storeys. The beams at the second and the third storeys were destroyed completely. Compared with the long standoff case, damage in the short standoff case was more localized.

7. CONCLUSIONS

In the seismic response to the long-distance MCE event at a soft soil site, the maximum base shear force coefficient reaches 13.9% which exceeds the notional horizontal load which is specified in the local building code as 1.5% of the characteristic dead weight of the building.

With regard to the response of an RC frame subjected to EIGMs, the following conclusions can be made:

- During Phase I, the high shear force may cause shear failure in members. As the deformation increases in Phase II, joint failure may take place due to a large inter-storey drift ratio.
- Current damage assessment techniques may not adequately reflect joint failure or shear failure phenomena occurring in members.

For the dynamic response of RC frames to external explosions, it has been observed that both the characteristics of dynamic response and damage levels depend on the standoff distance. Collapse mechanisms resulting from blast induced transient excitations require further in-depth studies.

REFERENCES

ABAQUS, 2001. *Standard User's Manual*, Version 6.2, HKS, Inc.

ASCE-ACI Joint Task Committee 426, 1973. "Shear Strength of Reinforced Concrete Members", *Journal of Structural Engineering*, ASCE, Vol. 99, No. 6, pp. 1091-1187.

Bardet, J. P., Ichii, K., and Lin, C. H., 2000. *EERA – A computer program for equivalent-linear earthquake site response analyses of layered soil deposits*, Department of Civil Engineering, University of Southern California, CA.

Dhakal, R. P., and Pan, T.-C., 2003. "Response Characteristics of Structures Subjected to Blasting Induced Ground Motions", *Journal of Impact Engineering*, Vol. 28, No. 8, pp. 813–828.

Hyder, D. W., 1991. "*ConWep: conventional weapons effects*", USAEWES / SS-R.

Karim, S. R., 1999. "Shear Strength Prediction for Concrete Members", *Journal of Structural Engineering*, ASCE, Vol. 125, No. 3, pp. 301-308

Li, B., Wu, Y. M., and Pan, T.-C., 2003. "Seismic Behavior of Non-

seismically Detailed Interior Beam-Wide Column Joints for Seismic Performance Part I: Experimental Results and Observed Behavior", ACI *Structural Journal*, Vol. 31, No. 8, pp. 1501–1523.

Ma, G., Hao, H., Lu, Y., and Zhou, Y. X., 2002. "Distributed Structural Damage Generated by High-Frequency Ground Motions", *Journal of Structural Engineering*, ASCE, Vol. 128, No. 3, pp. 390–399.

Megawati, K. and Pan, T.-C., 2002. "Prediction of the maximum credible ground motion in Singapore due to a great Sumatran subduction earthquake: the worst-case scenario", *J. Earthquake Engrg. Struct. Dyn*, 31, 1501-1523

Pan, T.-C., Dhakal, R. P., and Irawan, P., 2001. "*Dynamic and Pseudo-Dynamic tests of Lightly Reinforced Concrete Beam-Column Sub-Assemblies*", Technical Report No.2, Protective Technology Research Centre, School of Civil and Environmental Engineering, Nanyang Technological University.

Park, R., and Paulay, T., 1974. "*Reinforced Concrete Structures*", John Wiley and Sons.

Park, Y. J., and Ang, A. H.-S., 1985. "Mechanistic Seismic Damage Model for Reinforced Concrete Structures", *Journal of Structural Engineering*, ASCE, Vol. 111, No. 4, pp. 722-739.

Paulay, T., Park, R., and Priestley, M. J. N., 1978. "Reinforced Concrete Beam-Column Joints under Seismic Action", *ACI Journal*, Nov., pp. 585-593.

Pitts, J., 1984, "A review of geology and engineering geology of Singapore", *Quarterly Journal of Engineering Geology*, 17, pp. 93-101.

Priestley, M. N. J, Verma, R., and Xiao, Y., 1994. "Seismic Shear Strength of Reinforced Concrete Columns", *Journal of Structural Engineering*, ASCE, Vol. 120, No. 8, pp. 2310-2329.

Tregoning, P., Brunner, F. K., Bock, Y., Puntodewo, S. S. O., McCaffrey, R., Genrich, J. F., Calais, E., Rais, J., Subarya, C., 1994. "First Geodetic measurement of convergence across the Java Trench", *Geophysical Research Letters*, 21, 2135-2138.

Valles, R. E., Reinhorn, A. M., Kunnath, S. K., Li, C., and Madan, A., 1996. "*IDARC 2D Version 4.0: A Program for the Inelastic Damage Analysis of Buildings"*, Technical Report NCEER-96-0010, National Center for Earthquake Engineering Research, State University of New York at Buffalo.

Zachariasen, J., Sieh, K., Taylor, F. W., Edwards, R. L., and Hantoro, W. S., 1999. "Submergence and Uplift Associated with the Giant 1833 Sumatran Subduction Earthquake: evidence from coral micro atolls", *Journal of Geophysical Research*, 104, 895-919.